Statistical Characteristics of Aircraft Arrival Tracks

John F. Shortle*
Systems Engineering and Operations Research
Center for Air Transportation Systems Research
George Mason University
4400 University Dr., MS 4A6
Fairfax, VA 22030
Tel: 703-993-3571
Fax: 703-993-1521
e-mail: jshortle@gmu.edu

Yimin Zhang
George Mason University
4400 University Dr., MS 4A6
Fairfax, VA 22030
Fax: 703-993-1521
e-mail: yzhangk@gmu.edu

Juan Wang
George Mason University
4400 University Dr., MS 4A6
Fairfax, VA 22030
Fax: 703-993-1521
e-mail: jwangl@gmu.edu

* Corresponding author

Word Count: 4,830
Number of Figures: 10
Submission Date: 7/31/09

ABSTRACT

The statistical characterization of flight tracks is a critical component of some safety-analysis methods. This paper gives algorithms for obtaining statistical characteristics of aircraft arrival positions based on multilateration data. The algorithms organize the input data, consisting of observed aircraft positions, into arrival and departure tracks and parse the data to obtain separation times, lateral and vertical positions, and other associated data at various points along the approach path. Key results are the following. The smallest time separations observed are in the range of 50 – 60 seconds. The smallest separations in VMC are somewhat smaller than the smallest separations in IMC. The separation distribution does not appear to change much at different points along the approach path. The left tail of separation (corresponding to the smallest separation values) decays like a normal distribution and does not appear to be heavy-tailed. This is positive from a safety perspective. If we extrapolate this behavior beyond the observed data, we conjecture that smaller separations have extremely low probabilities that rapidly decay to effectively zero probability. Lateral positions near the threshold do not appear to be heavy-tailed either.

INTRODUCTION

The objective of this paper is to characterize statistical properties of aircraft flight tracks of arrivals to a major U.S. airport. A statistical characterization of aircraft flight tracks is useful for a variety of reasons.

First, the statistical distributions are critical in many quantitative safety analyses. For example, in the analysis of wake vortex encounters (e.g., *1*,*2*), the distribution of airplane locations is important for determining the fraction of flights that may encounter a wake vortex. Of particular importance is the *tail behavior* – that is, the extremely large values and/or the extremely small values of the distribution. For example, wake encounters are more likely to occur when the separation time is unusually small and/or when the trailing aircraft is at an unusually low altitude and/or when the leading aircraft is at an unusually high altitude (this is because wakes tend to sink). The “typical” or “average” values of the distribution typically do not drive the safety results. Rather, it is the values in the tail. If the extreme values of the distribution can be reduced or removed, then the safety of the system typically improves.

A second benefit of a statistical characterization of flight tracks is to identify potential benefits of various NextGen technologies. Many NextGen technologies seek to reduce the *variance* in aircraft positions. For example, required navigation performance (RNP) technologies seek to narrow the region of space centered about a target track in which the aircraft is likely to be found. Trajectory-based operations reduce the variability of separation in time by providing time requirements for passing certain waypoints, or by maintaining a specific separation behind a leading aircraft. A reduction in separation variance provides an indirect improvement in capacity. Because the extremely short separation times are eliminated, the target separation can be reduced, thus improving capacity, while maintaining or improving the existing level of safety.

Several researchers have measured the statistical distributions of aircraft separations on arrival, both in terms of distance and time. (*3*) and (*4*) measured the separation times by directly observing airport operations using a stopwatch. Others have obtained similar distributions using PDARS data (*5*), radar data (*6*) and multilateration data (*7*, *8*). This paper extends and revises the algorithms given in (*8*). Key contributions of this paper are that we provide algorithms for obtaining the *vertical* position of aircraft in addition to the lateral and longitudinal position, and we obtain results related to the extreme values of the distributions based on a larger volume of data. For rare-event probabilities for aircraft deviations in the en-route environment, see (*9*, *10*, *11*).

METHODOLOGY

Multilateration systems collect aircraft position data by computing the time difference of arrival of transponder signals to multiple receiving stations. The update rate is about once per second, significantly faster than the update rate of standard radar (once every 4+ seconds). Multilateration systems are part of some ASDE-X systems for alerting controllers to potential runway incursions. This paper utilizes multilateration data collected at Detroit Metropolitan Wayne County airport (DTW) during 2003. The data range extends to about 10 nm from the airport and also includes surface movements.

We now describe algorithms for processing multilateration data to obtain probability density functions (PDFs). In raw form, multilateration data consist of aircraft positions as a function of time. However, in our data source there is no indication that a particular data point is part of an arrival track or a departure track or a flyover, or which runway the aircraft is arriving to or departing from. A series of processing steps must be conducted to organize the data in order to recover higher-level information, such as the time separation between successive arrivals to a runway. These steps are as follows.

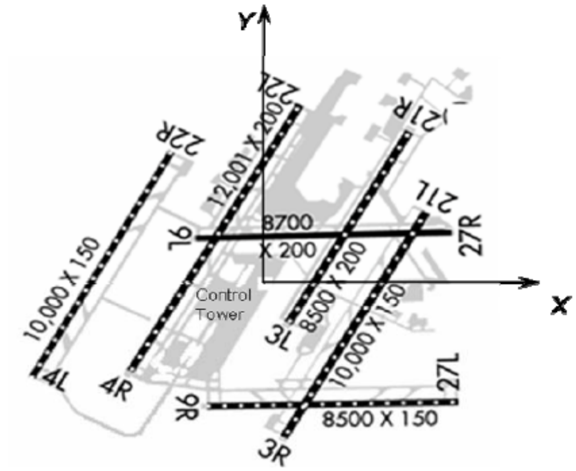

FIGURE 1: Diagram of DTW airport

__Step 1__: Conversion of Oracle dump files to text files. The original multilateration data files are Oracle dump files. We import the files into Oracle and export them as text files. This allows them to be easily read by common software programs such as Matlab, Word, Perl, and so forth. An input file consists of a single table with five fields. Each row in the table is copied to a row in the text file, subject to the changes described below.

- Aircraft mode-S. The mode-S value uniquely identifies a physical aircraft.
- Time. The input field is given in the format ‘yy/mmm/dd hh.mm.ss.000000 AM[PM]’ in GMT. In the output file, we convert time to seconds since midnight of the current day (in GMT).
- *x*-coordinate (meters). The *x*-axis is aligned with true east. The *y*-axis is aligned with true north. The origin of the coordinate system is the airport control tower (Figure 1).
- *y*-coordinate (meters).
- Mode-C. This field is a barometer-based value that can be used to estimate altitude.

__Step 2__: Rotation. The coordinates of the original multilateration data are aligned with true north and east. For analysis of a given runway, it is more efficient to use a rotated coordinate system where the *x*-axis is aligned with the runway. The required rotation angle α is the runway angle minus 90˚ minus 6.8˚, where 6.8˚ corresponds to the difference between true north and magnetic north. To illustrate, runway 21L has an angle of 215.5˚ relative to magnetic north. Its angle relative to true north (the *y*-axis in the original coordinate system) is 215.5˚ – 6.8˚ = 208.7˚. Its angle relative to true east (the *x*-axis in the original coordinate system) is 208.7˚ – 90˚ = 118.7˚. The rotation is performed via the following equations:

$$x_{new} = \cos(\alpha)\, x_{orig} - \sin(\alpha)\, y_{orig},$$
$$y_{new} = \sin(\alpha)\, x_{orig} + \cos(\alpha)\, y_{orig},$$

After rotating the coordinate points, we translate the coordinate system so that the origin is located at the threshold of the runway (as in Figure 2).

__Step 3__: Boxing. The multilateration data contain records associated with *all* aircraft in the vicinity of the airport. The objective of this step is to reduce the number of records to exclude points not associated with arrivals to a specific runway (say, 21L) or points far away from the threshold. To do this, we create two boxes near the runway of interest, as shown in Figure 2. All points that are outside of both boxes are discarded. This greatly reduces the number of data points that need to be processed in subsequent steps. Also, in this step, we convert the mode-C value to altitude via:

$$\text{Altitude (MSL) in meters} = (25 \times \text{Mode-C} - 10{,}000) \times .3048,$$

where .3048 converts feet to meters. Figure 2 shows the results of this step applied to a single day of data.

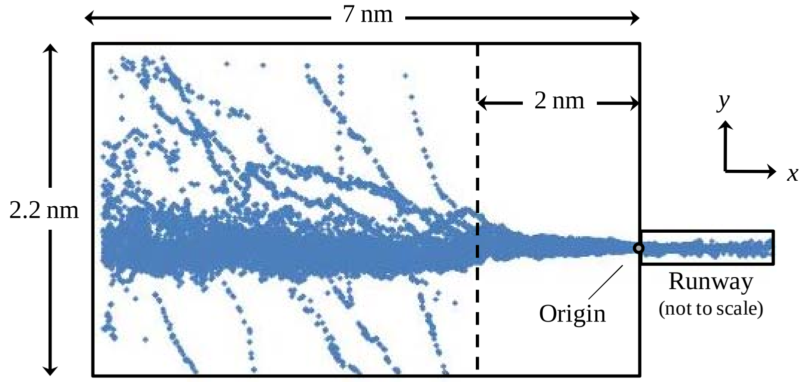

FIGURE 2: Boxed region of multilateration data

Step 4: Extract individual tracks. Roughly speaking, we define a "track" to be a set of points corresponding to one operation (an arrival or departure or possibly a go-around or flyover). At this point, the data consist of a long list of multilateration points, but there is no designation that any particular set of points should be grouped together to form a single operation. The objective of this step is to take the long list and identify break points where one track ends and another begins.

We first sort the boxed data (from Step 3) by mode-S and then by time. In this way, all points associated with a given physical aircraft are located together in the data set. A record is assumed to be the start of a new track if any of the three conditions holds:

1) Its mode-S value is different than the mode-S of the previous record, or
2) There is a time gap of more than 60 seconds from the previous record, or
3) There is a change in (non-vertical) distance greater than 0.4 nm from the previous record.

The last two steps assume that if there is a gap in time or distance between two successive measured positions of the same aircraft, then the two positions correspond to different operations. For example, this could correspond to an aircraft that departs the airspace then arrives a significant time later at a different position. These conditions can also be triggered by missing data. In such a case, one arrival may be split into two separate "tracks". In subsequent steps, these two "half-tracks" will be discarded due to data-integrity checks described later. The end effect is that these conditions ensure that no tracks have any gaps in time greater than 60 seconds or gaps in distance greater than 0.4 nm.

Step 5: Identify arrival tracks. Each data point contains a mode-S identifier which uniquely identifies a physical aircraft. However, it does not identify if the point is part of an arriving flight or a departing flight, nor does it identify the relevant runway. For example, there are points in Figure 2 that appear to be part of flyover tracks or operations on other runways. This step extracts only those tracks that correspond to arrivals at the selected runway. A track is considered an arrival if all of the following are true:

1) The first point of the track is at least 2 nm prior to the threshold (Figure 2),
2) The last point of the track is at least 0.15 nm beyond the threshold,
3) When the aircraft crosses the threshold of the runway, its lateral position is within the width of the runway.

The first two conditions identify arrivals versus departures and also ensure that the track has sufficient data and does not have gaps. The last condition helps to eliminate flyovers that happen, by chance, to satisfy the first two conditions.

Step 6: Adjust altitude measurements. The altitude measurements come from mode-C pressure measurements, rather than from multilateration data. This is because it is difficult to accurately triangulate the vertical position from ground sensors. However, the pressure measurements have a substantial amount of noise. This is illustrated in Figure 3, which shows the track of one sample landing. The black lines denote the original measurements. There are a number of missing or "zero" values. Also, some values appear to abruptly "pop up" or "pop down" from the true trajectory. It is non-trivial to determine which values are "bad" and which values are correct. We describe a heuristic which attempts to identify and correct the bad altitude measurements. The red line in the figure shows the result of this heuristic. Visually, it appears to provide a reasonable correction to the original data (the step-like behavior of the data is due to the discrete nature of the mode-C reading).

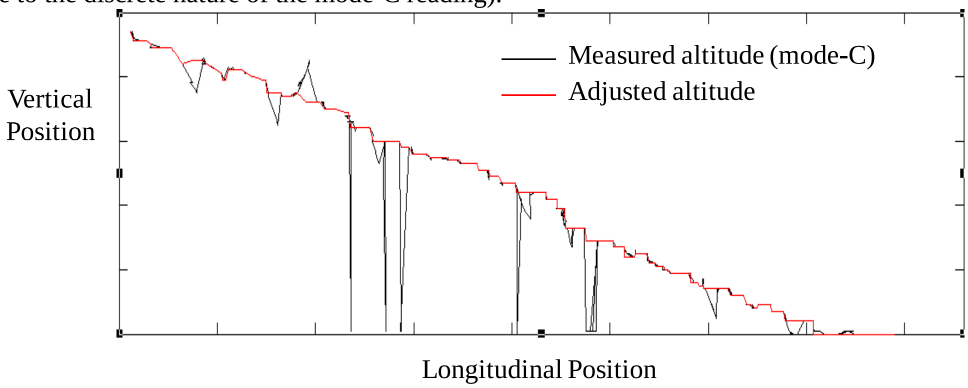

FIGURE 3: Corrected altitude measurements

The heuristic for correcting the bad altitude values is as follows:

1. If the track is missing *all* altitude values, we keep the track without any altitude information, since the lateral and longitudinal positions still provide useful information (say, for aircraft separation).
2. If the track is missing *some* altitude values, we eliminate those points from the track. We recheck that the revised track satisfies the conditions stated previously in Step 5. If not, the track is discarded.
3. We renormalize all altitude measurements so that the runway is at height 0. Specifically, the measured altitude when the airplane is on the runway is subtracted from every altitude measurement.
4. To eliminate the "bad" altitude values, we make two steps in order:
    a. For each point, if the altitude is more than 150 feet away from the average of the two adjacent points, then the point is discarded.
    b. For each point, if the slope of this point compared with the last valid point is greater than 0.2, then the point is discarded. (The idea is that abrupt changes in altitude are an indication of bad data).
5. The eliminated altitude values are replaced using linear interpolation using the nearest points with valid altitude values.

Step 7: Collect track statistics at a given longitudinal position. Each track represents a path in three dimensions $\{x(t), y(t), z(t)\}$. This step extracts the lateral and vertical position of the aircraft (y and z) as it crosses a given longitudinal position x. (This is done via interpolation when the individual track points do not lie exactly at the specified longitudinal position). The result is a "snapshot" of the aircraft positions at certain distances from the threshold. Finally, we can determine the time separation (at a given longitudinal position) by sorting the points according to time and computing the difference in time between two successive aircraft as they pass through the specified longitudinal position.

Step 8: Collect other track information. In this step, we collect other pieces of information associated with each track. These include:

- IMC/VMC. We determine whether or not an arrival was flown under IMC or VMC conditions using the IMC/VMC flag in the ASPM database. The ASPM data is linked to the multilateration data using the time and date fields (and by appropriately converting GMT to local time). Specifically, the time of the earliest data point in a given multilateration track is used as the linking key for the ASPM database.
- Wind speed and direction. This is obtained from the ASPM database in a similar manner.
- Average ground speed. Ground speed is computed as the distance between two multilateration records divided by the time difference between the records. Because of challenges in computing a derivative over small time scales, we use an average here. One point used in the speed calculation is the earliest point of the track that is within 100 ft of the centerline of the runway. The other point is the point where the aircraft crosses the threshold. The ground speed is the Euclidean distance between these points divided by the difference in time.
- Average air speed. Air speed is computed by appropriately combining the ground speed and the component of wind speed aligned in the direction of the runway.

As a validation check, Figure 4 shows a comparison of the arrival counts observed in the ASPM database and the arrival counts observed from the multilateration data. (ASPM provides a total arrival count for all runway. To compare against the multilateration counts, we analyze the arrival tracks of all six runways in both directions and sum up the total number of arrivals). There are two key observations from the figure. First, the multilateration counts are less than the ASPM counts. This is expected. We deliberately designed the multilateration processing algorithms to remove tracks that fail any of a number of data integrity checks (e.g., missing data, noisy data, etc.). Thus, we expect to remove a certain number of multilateration tracks in order to ensure that the remaining tracks pass a data quality threshold. Second, there is still agreement between the *timing* of the two data series (that is, where the peaks and valleys lie). The main purpose of this exercise is to validate that the linking of the two datasets via the date/time field is correct. Thus, we can be confident that each multilateration track is appropriately matched with the fields pulled from the ASPM database (e.g., IMC/VMC).

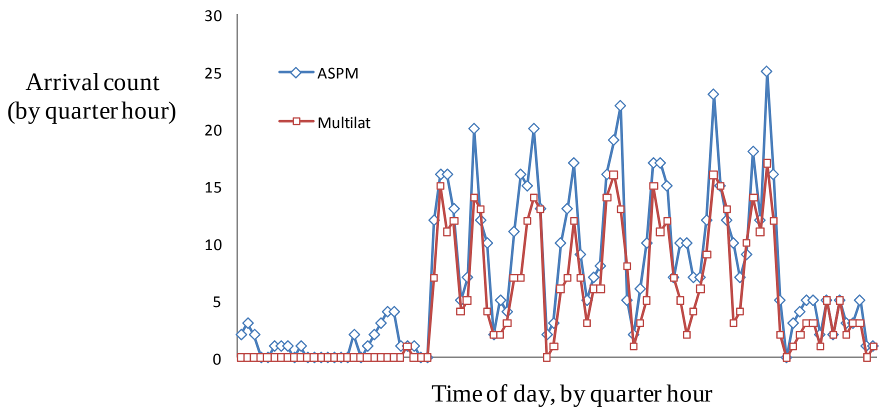

FIGURE 4: Comparison of ASPM and multilateration arrival counts

RESULTS

The results in this section are based on two months of arrival data (Jan. – Feb. 2003) on runway 21L. The total number of valid tracks obtained over this period of time is about 8,000 (roughly 2,500 during IMC and 5,500 during VMC). Note that many tracks are thrown away due to data integrity issues, so these numbers represent lower bounds on the actual number of arrivals during these two months.

Figure 5 shows the distribution of separation at the threshold, broken down by VMC and IMC arrivals. As might be expected, the VMC separations are slightly smaller than the IMC separations. The smallest separations observed are around 50 or 60 seconds. The separations on the left-tail of the distribution are the most important from a safety perspective, since they correspond to situations in which the aircraft are most closely separated. The separations on the right-tail of the distribution are of less interest in this paper. They correspond to natural gaps in the arrival pattern and may be of interest from a capacity-utilization perspective.

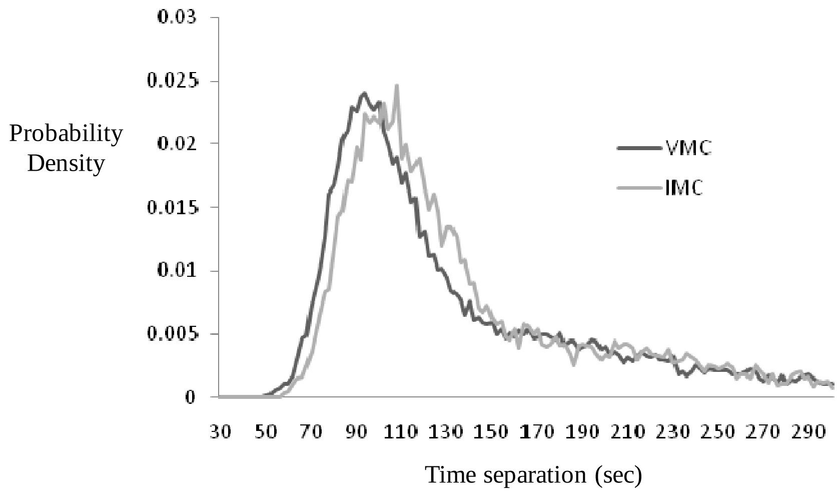

FIGURE 5: Time separation distribution

Figure 6 shows how the separation distribution varies in terms of distance to the threshold. The dot is the median observation. The box specifies the 25% quantile and the 75% quantile. The size of the box is defined as the inter-quartile range. As the aircraft get closer to the runway, there is a slight increase in the median separation distance and a slight increase in the size of the inter-quartile range (denoting a slight increase in separation variability as aircraft get closer to the threshold). However, these differences are somewhat minor and a statistical test does not reject the hypothesis that the distributions are the same. Thus, the separation distribution at the threshold adequately represents the separation distribution at various points along the approach path. (In the figure, the upper adjacent value is the largest observation that is less than or equal to the upper quartile plus 1.5*r*, where *r* is the inter-quartile range. The lower adjacent value is the smallest observation that is greater than or equal to the lower quartile minus 1.5*r*. The outliers, beyond the adjacent values, tell the extreme value of the distribution.)

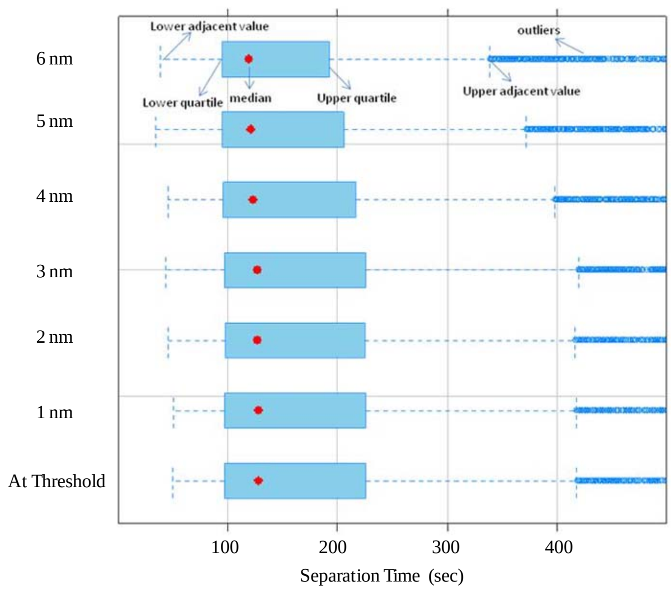

FIGURE 6: Time separation at various distances from threshold (VMC and IMC)

Figure 7 shows the lateral and vertical components of position as a function of the distance to the threshold. As expected, the variability rapidly decreases as aircraft get closer to the runway. The correlation coefficient (between the lateral and vertical positions) ranges from -.02 to .13 for all of the distances to the threshold. Thus, for practical purposes, the lateral and vertical deviations can be assumed to be independent.

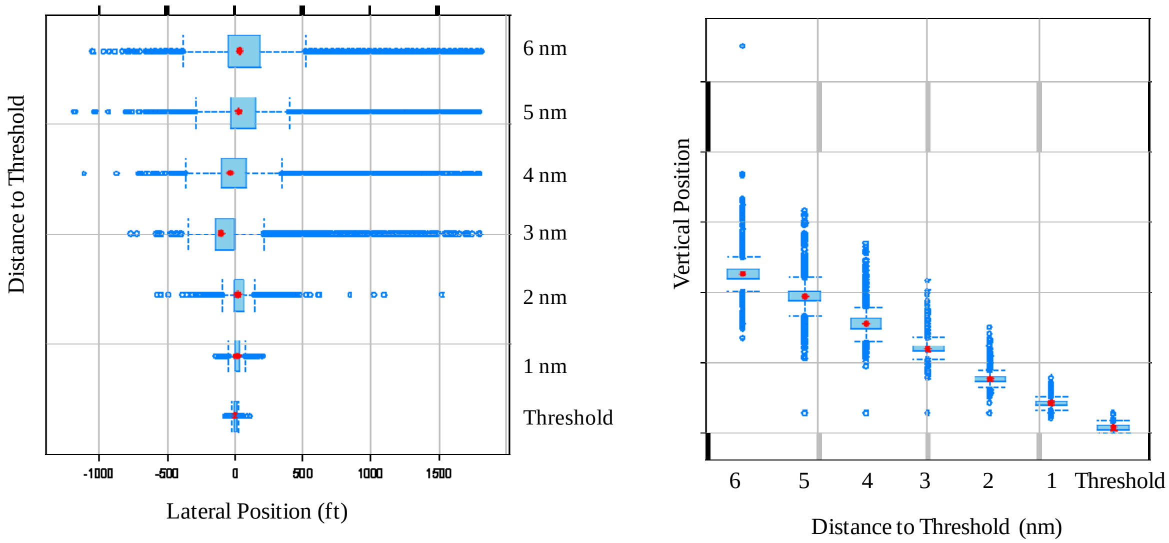

FIGURE 7: Lateral and vertical position (VMC and IMC)

The left side of Figure 8 shows a top-level view of flight tracks for one day of data. The points are color-coded based on weather conditions (IMC or VMC). In IMC, aircraft fly through the final approach fix straight to the runway. In VMC, it is possible for aircraft to curve in from the side without flying directly through the fix. The tracks in the figure are consistent with these rules, though there do appear to be occasional tracks in IMC that come in from the side without flying through the fix. The right figure shows the sample PDF of the lateral position (based on the entire data set, not just one day) at a point 4 nm from the runway. The right tail of the distribution is “fatter” during VMC corresponding to the tracks that curve in from the side. Similar symmetric results hold for the parallel runway (21R) in which the tracks curve in form the other side.

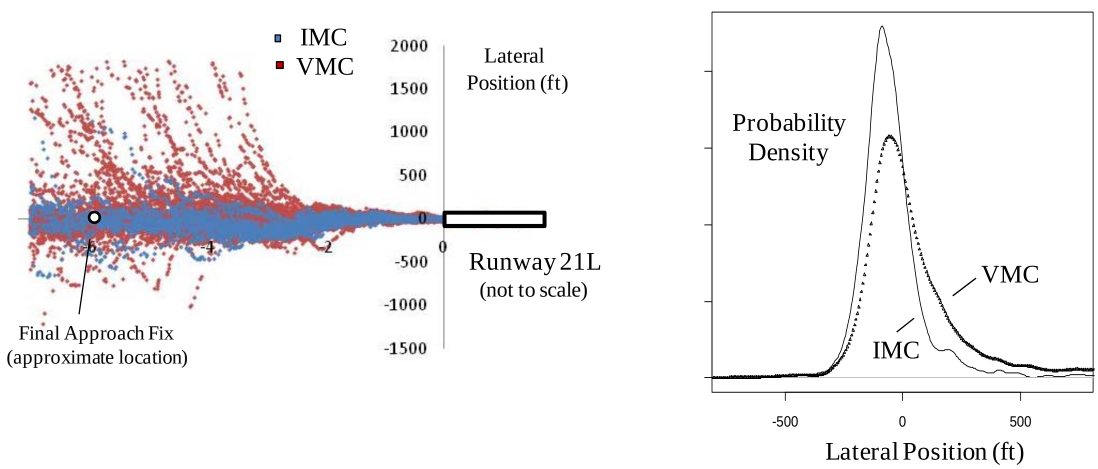

FIGURE 8: Lateral position of aircraft

We now investigate the tail behavior of the distributions. The tail behavior is critical from a safety perspective, since it governs the frequency with which extremely large or extremely small values are observed. Further, different kinds of distributions yield vastly different extreme-event probabilities, so it is important to classify the tail behavior well.

A commonly used distribution is the *normal* distribution, since it governs statistical patterns frequently observed in daily life. For example, human heights are approximately normally distributed. From a rare-events perspective, the normal distribution is said to be *light-tailed*. Intuitively, this means that the probability of finding a very tall person – say, someone 50% taller than average (about 8 feet tall) – is extremely small. The probability of finding someone just a little bit taller – say, 60% taller than average – is even much smaller. In other words, the probability drops off very rapidly as the value in question gets larger and larger.

A critical question from a safety perspective is: Do aircraft positions follow the same normally-distributed behavior? In other words, does the probability of observing an extreme event decay very rapidly as one gets further from the average? Or more practically, how often might we expect to observe extremely short separations (say, 30 seconds apart)? Do such events occur with effectively zero probability or do they occur with some small, but non-trivial, probability? These are the kinds of questions we are trying to answer by looking at the tail behavior.

In contrast to the normal distribution are distributions that decay according to a power law (these are said to be *heavy-tailed*). An example is the Pareto distribution. Examples of power law distributions are file sizes on the Internet and insurance claim sizes. In these examples, it is not uncommon to observe extremely large values that are much greater than the mean – for example, an insurance claim that is 10 times the average. In contrast, for a light-tailed distribution like human height, it is impossible to observe a value 10 times the mean.

The tail behavior of a distribution is described by its cumulative distribution function (CDF) $F(x)$ or by its complementary CDF (CCDF) $F^c(x) = 1 - F(x)$. Some common distributions and their associated tail decay rates are:

- Normal-distribution decay: $F^c(x) \sim c \exp(-ax^2)$,
- Exponential decay: $F^c(x) \sim c \exp(-ax)$,
- Power-law decay: $F^c(x) \sim c\, x^{-a}$,

where a and c are constants. The symbol '~' denotes that for large x, the function on the left looks like the function on the right. Mathematically, $f(x) \sim g(x)$ if $f(x) / g(x)$ goes to 1 as x goes to infinity. Of these three distributions, the normal distribution has the lightest tail, and the power-law has the heaviest tail. The normal distribution is most desirable from a safety perspective and the power-law is the least desirable.

We can roughly determine the rate of decay by plotting the sample CDF or CCDF of the distribution and noting the shape. In particular, certain transformations of each distribution lead to a linear relationship. Creating the desired plot and checking for linearity in the extreme values gives a rough way to characterize the tail behavior. For example, the CCDF of an exponential distribution is $F^c(x) \sim \exp(-ax)$. Taking the natural log of both sides gives $\ln[F^c(x)] \sim -ax$. So, a plot of $\ln[F^c(x)]$ versus x yields a straight line. Similarly, for power-law decay, a plot of $\ln[F^c(x)]$ versus $\ln[x]$ gives a straight line asymptotically. For a normal-distribution decay, a plot of $\ln[-\ln[F^c(x)]]$ versus $\ln[x]$ gives a straight line asymptotically. The basic approach here is to take the distribution of interest, create each of the plots described, and then decide which plot looks most like a straight line in the tails.

For space reasons, we do not show all plots of all distributions here. Rather, we show a few representative plots and summarize the results:

- The left tail of separation time roughly follows a normal decay. This is shown by the (roughly) linear behavior of Figure 9 (which plots $\ln[-\ln[F(t)]]$ versus $\ln[t]$).
- The left and right tails of the lateral position follow exponential decay. This is shown by the linear behavior in the left and right sides of both graphs in Figure 10 (which plot $\ln[F(y)]]$ and $\ln[F^c(y)]]$ versus $\ln[y]$). (This does not imply that the entire distribution of lateral position is an exponential distribution, but rather that the extreme left and right values follow exponential decay like an exponential distribution. That is, we are commenting on the tail behavior of the distributions here, not on the shape of the "body" of the distribution.)

Neither distribution appears to have a power tail. This is positive from a safety perspective, because it means that larger lateral deviations or shorter separation times are extremely rare and can rapidly approach a point where the probability is effectively zero. Also, this asymptotic tail behavior is consistent with results for altitude deviations en-route (*11*) in which the decay rate is estimated to be between exponential and normal.

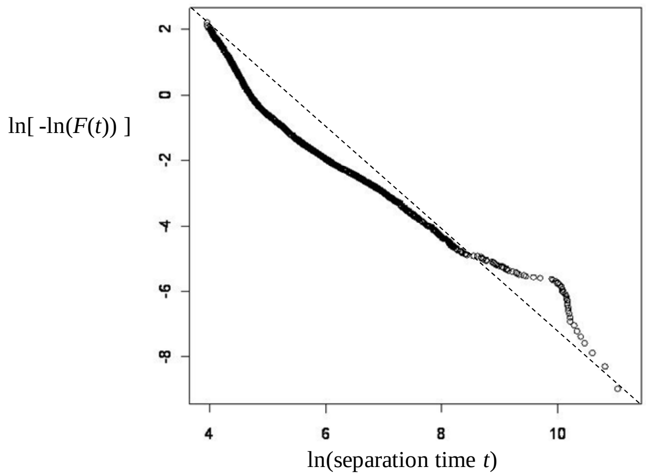

FIGURE 9: Left-tail of separation time follows a normal-like decay (1 nm from threshold).

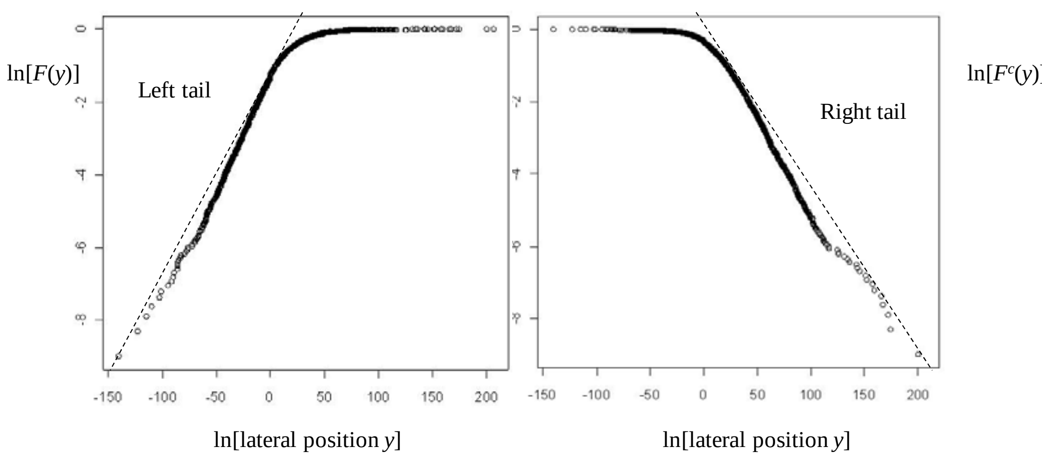

FIGURE 10: Left and right tail of lateral position follow exponential decay (1 nm from threshold).
[Note: x-axis should be just 'lateral position y']

CONCLUSIONS

This paper gave algorithms for obtaining higher-level statistical information about aircraft positions via the processing of multilateration data. The algorithms are fairly quick and can process one month of data in less than two hours on a standard PC. The statistical characterization of flight tracks is a critical component of safety-analysis models. Key results from analysis of two months of arrivals at a single runway are the following. The smallest time separations observed are in the range of 50 – 60 seconds. The smallest separations in VMC are somewhat smaller than the smallest separations in IMC. The separation distribution does not appear to change much at different points along the approach path. The left tail of separation (corresponding to the smallest separation values) decays like a normal distribution and does not appear to be heavy-tailed. This is positive from a safety perspective. If we extrapolate this behavior beyond the observed data, we conjecture that smaller separations have extremely low probabilities that rapidly decay to effectively zero probability. Lateral positions near the threshold do not appear to be heavy-tailed either, but exhibit exponential decay (somewhat slower than the decay of a normal distribution, but not heavy-tailed). Observed lateral positions are consistent with the fact that aircraft fly through the final approach fix in IMC, but not necessarily in VMC. Future work will involve integrating these distributions into probabilistic models of wake vortex behavior and carrying out an associated wake-vortex safety analysis.

ACKNOWLEDGEMENTS

This work has been supported by NASA and Northwest Research Associates (NWRA) through sub-agreement #NWRA-08-S-114.

REFERENCES

1. Shortle, J., B. Jeddi. 2007. Using multilateration data in probabilistic analysis of wake vortex hazards for landing aircraft. *Transportation Research Record: Journal of the Transportation Research Board.* No. 2007, 90-96.
2. Shortle, J. 2007. A comparison of wake-vortex models for use in probabilistic aviation safety analysis. In *Proceedings of the International System Safety Conference*, A. G. Boyer, N. J. Gauthier (eds.), Baltimore, MD, 581-589.
3. Haynie, C. An Investigation of Capacity and Safety in Near-terminal Airspace Guiding Information Technology Adoption. Ph.D. Dissertation, George Mason University, Fairfax, VA, 2002.
4. Xie, Y. Quantitative Analysis of Airport Arrival Capacity and Arrival Safety using Stochastic Models. Ph.D. Dissertation, George Mason University, Fairfax, VA, 2005.
5. Rakas, J., and H. Yin. Statistical Modeling and Analysis of Landing Time Intervals: Case Study of Los Angeles International Airport, California. In *Transportation Research Record: Journal of the Transportation Research Board*, *No. 1915*, TRB, National Research Council, Washington, D.C., 2005, pp. 69-78.
6. Ballin, M., and H. Erzberger. An Analysis of Landing Rates and Separations at the Dallas / Fort Worth International Airport. NASA Technical Memorandum 110397, 1996.
7. Levy, B., J. Legge, and M. Romano. Opportunities for Improvements in Simple Models for Estimating Runway Capacity, 23rd Digital Avionics Systems Conference, Salt Lake City, UT, 2004.
8. Jeddi, B., J. Shortle, and L. Sherry. Statistics of the Approach Process at Detroit Metropolitan Wayne County Airport. In *Proceedings of the International Conference on Research in Air Transportation*, Belgrade, Serbia and Montenegro, 2006, pp. 85-92.
9. Harrison, D. 1987. Some preliminary results of estimating the probability of vertical overlap from the distribution of single aircraft deviations from North Atlantic Traffic. UK CAA report.
10. Campos, L., J. Marques. 2002. On safety metrics related to aircraft separation. *Journal of the Royal Naval Society*, 55:39-63.
11. Campos, L., J. Marques. 2004. On a combination of gamma and generalized error distributions with applications to flight path deviations. *Communications in Statistics: Theory and Methods*, 33(10): 2307-2332.